

Development of a Large Format Fully Sampled Bolometer Camera for 2 mm Wavelength

Dominic J. Benford¹, Johannes G. Staguhn^{1,2}, Christine A. Allen¹,
Troy J. Ames¹, Ernest D. Buchanan^{1,3}, Stephen F. Maher^{1,4},
S. Harvey Moseley¹, Elmer H. Sharp^{1,5}, Edward J. Wollack¹

1 – NASA / Goddard Space Flight Center, Greenbelt, MD 20771 USA

2 – University of Maryland, College Park, MD 20742 USA

3 – AdNet Systems, Rockville, MD 20852 USA

4 – SSAI, Lanham, MD 20706 USA

5 – GS&T, Greenbelt, MD 20770 USA

ABSTRACT

The 2 mm (150 GHz) atmospheric window enables unparalleled ground-based observations of the earliest active dusty galaxies in the universe. We have undertaken the development of a bolometer camera, GISMO (the Goddard-IRAM Superconducting 2-Millimeter Observer), which will obtain large and sensitive sky maps at this wavelength. The instrument will be used at the IRAM 30 m telescope, where we hope to have a trial observing run in Summer 2007. The innovative element in this camera is its 8×16 fully sampled planar array of multiplexed superconducting transition edge sensor bolometers. This array is based on our recently demonstrated Backshort Under Grid architecture, designed to be scaled to kilopixel arrays with high sensitivity (of around $4 \cdot 10^{-17}$ W/ $\sqrt{\text{Hz}}$ at $T_c \sim 450$ mK). A compact cryogenic optical system provides a wide field of view of almost $2' \times 4'$, enabling GISMO to be very efficient at detecting sources serendipitously in large sky surveys, while retaining diffraction-limited imaging performance. GISMO will provide significantly greater imaging sensitivity and mapping speed at this wavelength than has previously been possible. The major scientific driver for the instrument is to detect dust emission from high- z ULIRGs and quasars. The instrument provides an important portion of the spectrum of high redshift galaxies at the Rayleigh-Jeans part of the dust emission spectrum, even at the highest redshifts. Models of galaxy evolution predict that GISMO will serendipitously detect one galaxy in every four hours of observing blank sky, and that one quarter of these galaxies will be at a redshift of $z > 6.5$.

1. BACKGROUND

A key observational tool in the study of the evolution of the universe out to cosmological distances is to observe the (redshifted) thermal emission from interstellar dust in galaxies. The most distant astronomical objects known to date are luminous, dusty galaxies at redshifts $z \sim 6$, a time when the universe was less than one Gyr old. At this epoch, the reionization of the universe was still not completed. These dusty galaxies all experience a phase of violent star formation, and a large number of them are seen to host luminous active nuclei (quasars) – processes that ultimately will reionize the universe. One of the major scientific pursuits for understanding the formation of structure in the universe is to learn about the physics of the formation of these galaxies. We would like to understand the relationship between the star formation and quasar activity with their corresponding feedback mechanisms in these objects. The bulk of the total luminosity of both processes in these dusty galaxies is redshifted into the submillimeter and millimeter regime and therefore can be efficiently observed at these wavelengths.

2. GISMO: A 2 MM BOLOMETER CAMERA FOR THE IRAM 30 M TELESCOPE

At NASA's Goddard Space Flight Center we are now building the bolometer camera GISMO (Goddard-IRAM Superconducting 2-Millimeter Observer), optimized for operating in the 2 mm atmospheric window. We have negotiated an opportunity to operate the instrument on the IRAM 30 m telescope on Pico Veleta in Spain (Baars et al. 1987). The instrument is primarily aimed at surveying the first dusty galaxies in the universe. The camera is built around an

8×16 pixel array of 2 mm pitch, close-packed superconducting Transition Edge Sensor (TES) bolometers which will be described in more detail in the following chapter. In this section, we discuss the scientific motivation for GISMO.

Continuum measurements of galaxies at long wavelengths are well suited to determining the luminosity and star formation rate in these objects (for a review see, e.g., Blain et al. 2002). Observations with GISMO will complement existing 850 μm – 1.25 mm SEDs of high redshift galaxies at the Rayleigh-Jeans part of the dust emission spectrum, even at the highest redshifts. In particular at redshifts of $z > 5$ sky-background-limited bolometric observations at 2 mm are highly efficient as compared to observations at shorter (sub)millimeter wavelengths. Figure 1 demonstrates this by showing a plot of the 1.2 mm/2.0 mm flux density ratio versus redshift for template LIRGs and ULIRGs with luminosities ranging between $L_{\text{FIR}} = 10^{11} L_{\odot}$ and $L_{\text{FIR}} = 10^{14} L_{\odot}$. With GISMO operating at 2 mm wavelength, three atmospheric windows will then be available for efficient continuum observations of the high- z universe: 2mm with GISMO; 1.2 mm with MAMBO (Kreysa et al. 2002) and Bolocam (Glenn et al. 2003); and soon 0.85 mm with SCUBA-2 (Holland et al. 2006). With the availability of three (sub)millimeter colors the accuracy in the determination of photometric redshifts and absolute luminosities for those objects will be improved. GISMO's pixel separation of 2 mm corresponds to an angular separation of 14" on the sky, or $\sim \lambda/D$ (only slightly beam oversampled) at 2 mm wavelength and the telescope diameter of 30 m. With this spatial sampling GISMO will be very efficient at detecting sources serendipitously in large sky surveys, while the capability for diffraction limited observations is preserved (Bernstein 2002). Dithering will be used to recover the full angular resolution provided by the telescope. Figure 2 shows our model predictions for the cumulative dark sky galaxy number counts versus flux for GISMO. Using the sensitivity numbers shown in Table 1 we find that we expect one 5σ galaxy detection on the blank sky in 4 hours of observing time, with the probability of 1 in 4 that it is at a redshift $z > 6.5$. Since the current highest quasar redshift is $z=6.42$ (Willott, McClure & Jarvis 2003), GISMO will be a powerful surveyor of the highest redshift universe.

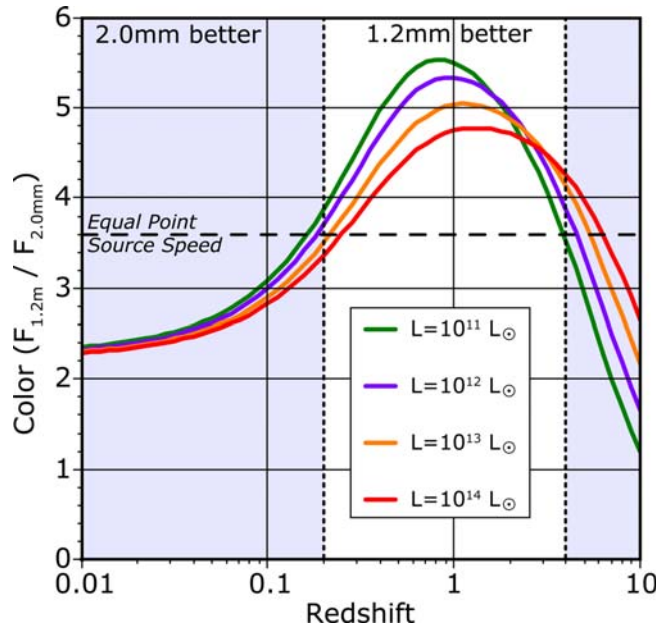


Figure 1. The modeled color (flux density ratio) between 1.2mm and 2.0mm as a function of redshift shows a significant change around redshifts of $z \sim 1$. For typical observing conditions, the color that provides equal point source signal-to-noise in equal integration time at both wavelengths is around 3.6 (dashed line). At typical galaxy luminosities, the plot shows that observations at a wavelength of 2.0mm are more sensitive than 1.2mm for detecting both local ($z < 0.2$) and very high redshift ($z > 4$) galaxies. When field of view is taken into account, the 2.0mm band is always favorable to the 1.2mm band.

The 2 mm spectral range provides a unique low background window through the earth's atmosphere (see Figure 3 and Table 1 which show sky parameters for Pico Veleta). However, in order to obtain close to sky background limited performance for a bolometer camera with 20% bandwidth operating at 2 mm wavelength, detectors with a noise

equivalent power (NEP) of $\approx 4 \cdot 10^{-17}$ W/ $\sqrt{\text{Hz}}$ or better are required to keep bolometer excess noise below 25%. A camera achieving this sensitivity can then conduct efficient observations of the earliest active dusty galaxies in the universe.

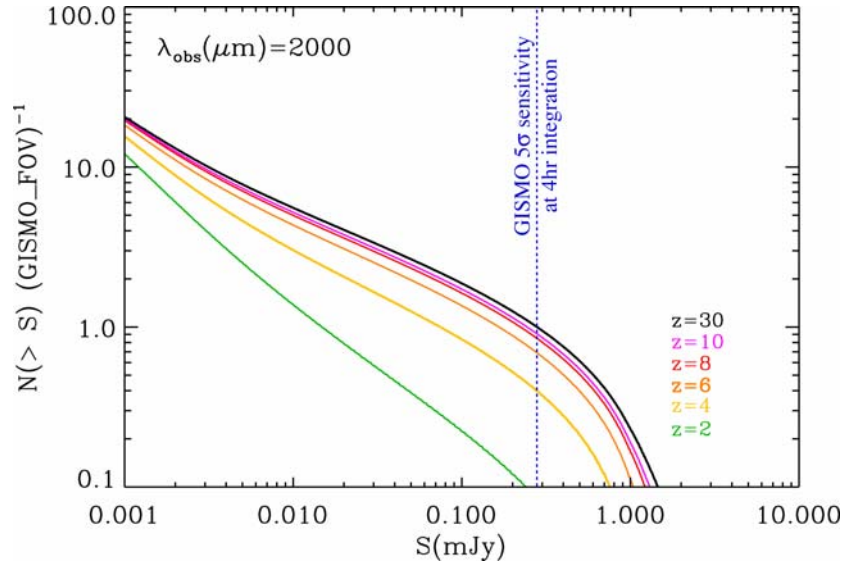


Figure 2. Model predictions for the cumulative dark sky galaxy number counts versus flux for GISMO. Each curve gives the number of sources per GISMO field of view at a redshift of less than the cutoff that is brighter than the indicated flux density.

Table 1. Typical winter and summer sky background at Pico Veleta.

Frequency (GHz)	Sky Emissivity	Sky Noise (W/ $\sqrt{\text{Hz}}$)	NEFD (mJy/ $\sqrt{\text{Hz}}$)
150 (2mm)	0.08 (Winter)	$5.5 \cdot 10^{-17}$ at Zenith	3.3
250 (1.2mm)	0.16 (Winter)	$2.4 \cdot 10^{-16}$ at Zenith	14
150 (2mm)	0.22 (Summer)	$1.4 \cdot 10^{-16}$ at 30° El.	10.5
250 (1.2mm)	0.45 (Summer)	$6.0 \cdot 10^{-16}$ at 30° El.	61

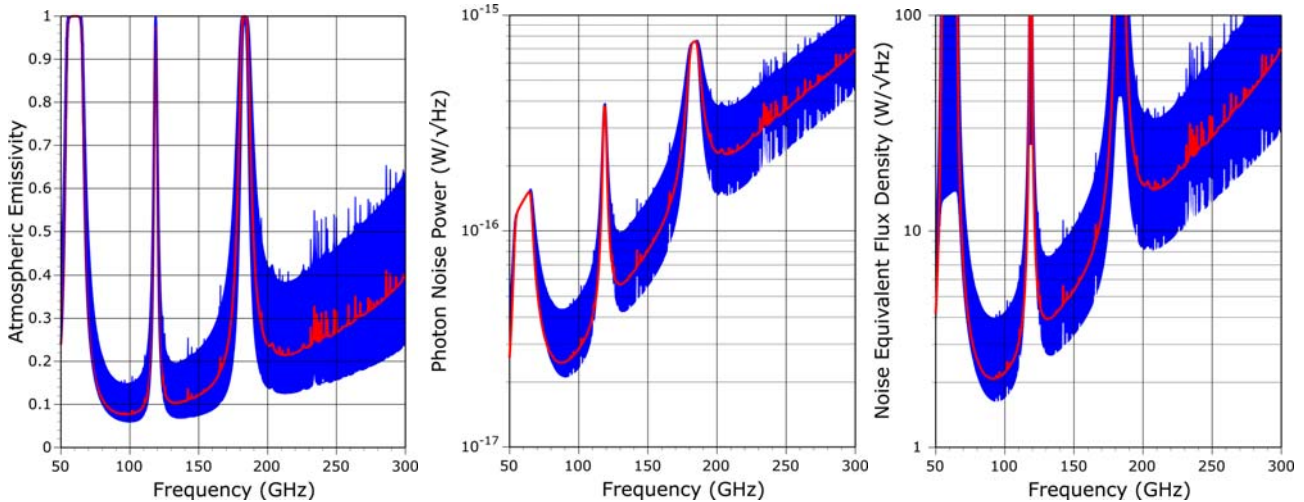


Figure 3. (Left) Modeled atmospheric emissivity as a function of frequency, showing a range of conditions between at the zenith in winter and at 30° elevation in summer; (Center) atmospheric photon noise for these conditions; (Right) noise equivalent flux density.

Other scientific projects for GISMO include – but are far from being limited to – large scale surveys of dust in protostellar clouds and galactic and extragalactic star forming regions.

3. DETECTORS: THE BACKSHORT-UNDER-GRID (BUG) ARRAY

We have developed a new type of two-dimensional planar bolometer array architecture, which separates the absorber and the backshort production, allowing a straightforward way to provide detector arrays for a wide range of wavelengths (Allen et al. 2006). The Backshort Under Grid (BUG) approach is comprised of a large array of thin membrane absorbers with leg thermal isolation (Figure 4, left). These photos show an enlargement of one pixel which shows the integrated Transition Edge Sensor (TES) bolometer in more detail. The normal metal “Zebra” structure on the Mo/Au thermistor, which is used to suppress excess noise (Staguhn et al. 2004), is clearly visible in this image. An 8×16 array will be used in GISMO. Figure 4 (center) shows an image of this BUG array, fabricated in our group at NASA/GSFC.

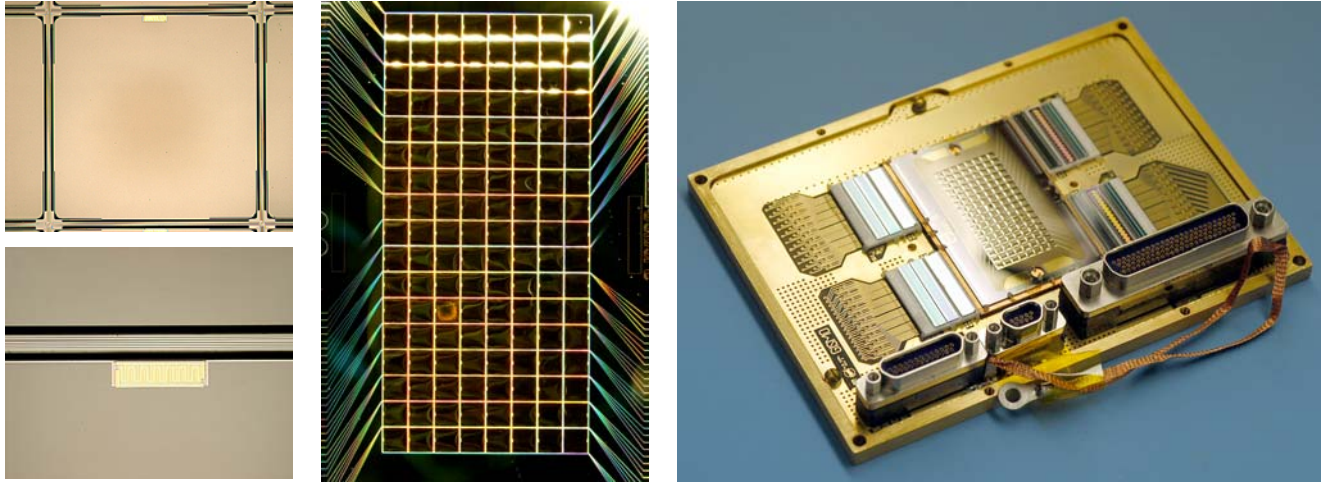


Figure 4. (Left): These photos detail the individual bolometer construction, including the eight thermal isolation legs and the thermistor with interdigitated noise suppression normal metal bars; (Center): Photograph of the completed 8×16 array of 2mm-pitch pixels; (Right): The GISMO detector package, providing four readout columns each with a (from outside to inside) SQUID multiplexer chip, Nyquist Inductor chip, and Shunt chip; the micro-D connectors at the lower edge set the overall size of the box, which is around 88 mm \times 120 mm.

The TES arrays are read out by four 32-channel SQUID time-domain multiplexers provided by NIST/Boulder (deKorte et al. 2003). Both the readout electronics (Forgione et al. 2004) and the IRC control and data acquisition software (Ames & Case 2003) are used in other instruments such as the MUSTANG 3 mm bolometer camera for the Green Bank Telescope (Dicker et al. 2004). The complete array package with biasing shunt resistor chips, Nyquist inductor filter chips, and SQUID multiplexer chips, is shown in Figure 4 (right).

Individual bolometer characteristics were determined by precise measurements on small witness sample of four bolometers each. The phonon noise equivalent power (NEP) of the bolometers is $4.2 \cdot 10^{-17}$ W/ $\sqrt{\text{Hz}}$, which is comfortably less than the expected sky noise of $\sim 8 \cdot 10^{-17}$ W/ $\sqrt{\text{Hz}}$ (Figure 3). A reduction in the transition temperature (the tested device has $T_C = 459$ mK) could be used to further improve the detector noise without any modification of the array design, since the GISMO refrigerator – a $^3\text{He}/^4\text{He}$ system (from Chase Cryogenics, www.chasecryogenics.com) with a base temperature of below 260 mK – will allow the operation of bolometers with T_C of below 400 mK). However, this reduction in noise is accompanied by a reduction in saturation power, and for instrument validation under mediocre weather conditions and lower elevations, a saturation power of well above 20 pW is needed; given this, a T_C of at least 430 mK is required, allowing only 15% reduction in phonon noise.

We measured an electrothermal feedback time constant, τ_{eff} , of about 50 μs ($F_{TES} \sim 3.5$ kHz). The detector circuit contains a Nyquist inductor which is chosen such that the detector integrates for a full readout cycle of the multiplexer (typically the frame rate is set to around 10 kHz). A measured noise spectrum of a representative bolometer was published by Staguhn et al. (2006). The measured in-band noise of the device on at two bias points is less than 20%

above the fundamental phonon noise limit. Only the out-of-band (>3 kHz) excess noise is higher than this value. This noise is suppressed by the Nyquist filter and therefore does not degrade the overall performance.

In recent optical tests, a small aperture was placed in the cryostat to limit power on the detectors (in part to enable viewing of a room-temperature blackbody without saturation). This also provided a variation in the power on each detector. A current-voltage curve taken on many detectors simultaneously is then representative of a family of such curves taken on a single device taken at many different illuminations. In Figure 5 we show a family of simultaneous measurements, both in bias current vs. voltage and bias power vs. voltage. Note that the current is very nearly hyperbolic (i.e., constant power) when on the superconducting transition, whereas the current is highly linear (i.e., constant resistance) when in the normal regime. The measured resistances of all bolometers has a distribution that is approximately Gaussian with a standard deviation of 2%. Due to the aperture, the powers on the transition vary; under the assumption that the saturation power of 30 pW is identical for each detector (which is approximately true), the optical power is then just the difference between this and the measured bias power for each detector, or 13 to 20 pW.

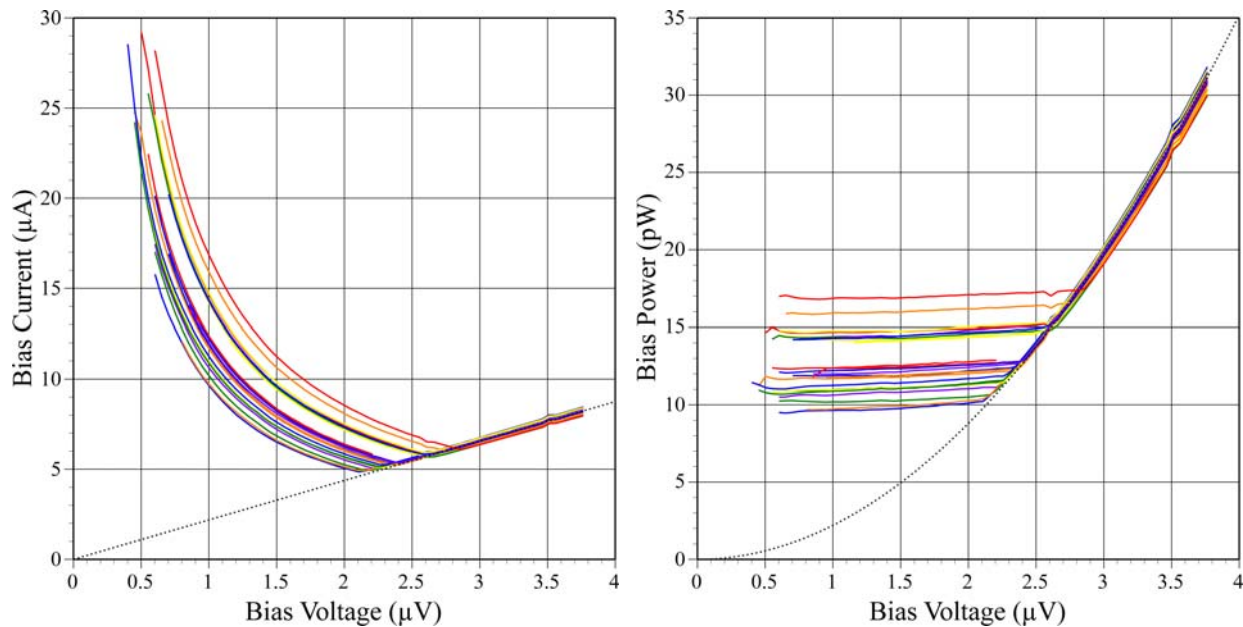


Figure 5. (Left) Measured current vs. bias voltage for an array of bolometers; (Right) Calculated bias power vs. bias voltage. Note that the detectors were illuminated by different powers, and hence the curves do not overlap.

Initial optical tests used an internal blackbody calibration source to illuminate the bolometers. A representative graph of the received power as a function of the illuminator temperature is shown in Figure 6. The curve can be fit to the expected power of the blackbody and is nearly linear, with a typical R^2 of >0.98 and an offset of always <1 pW. Further optical testing was conducted with the cryostat window open, to verify the beam outside the cryostat and to look for modulated signals from the far field. In Figure 6 is a time series of several detectors as one of us (EHS) waved his hand in the beam. Quantitatively, the beam appears to be of the correct size and with a $\sim 20\%$ hot spillover component consistent with diffraction around the internal aperture.

5. SUMMARY

We have built a 2 mm bolometer camera for the efficient detection of extremely high redshift galaxies. The camera is currently undergoing a variety of optical performance tests and our goal is the deployment of GISMO at the IRAM 30m telescope for trial observations in late 2007.

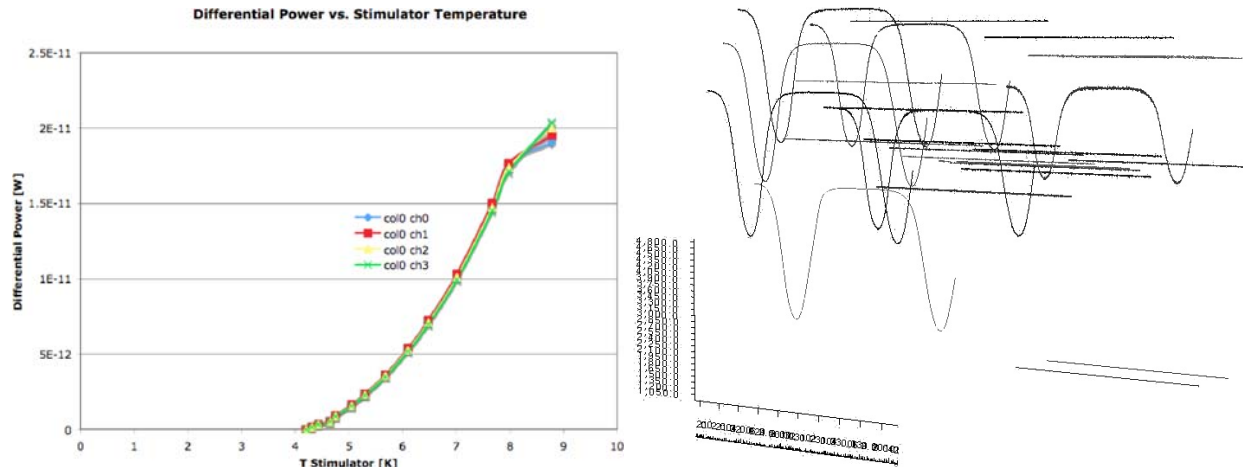


Figure 6. (Left) Detector optical power for several bolometers as a function of blackbody illumination temperature; (Right) Time series of the optical response to a warm source waved into and out of the beam (negative indicates more power).

REFERENCES

- Allen, C.A., Benford, D.K., Chervenak, J.A., Chuss, D.T., Miller, T.M., Moseley, S.H., Staguhn, J.G., Wollack, E.J., 2006, *Nuc. Inst. & Meth. Phys. Res. A*, 559, pp.522-524; “Backshort-Under-Grid arrays for infrared astronomy”
- Ames, T.J. & Case, L., 2003, *Proc. SPIE #4857*, pp.73-84; “Distributed framework for dynamic telescope and instrument control”
- Baars, J.W.M., Hooghoudt, B.G., Mezger, P.G. & de Jonge, M.J. 1987, *A&A*, 175, pp.319-326; “The IRAM 30-m millimeter radio telescope on Pico Veleta, Spain”
- Bernstein, G. 2002, *PASP*, 114, pp.98-111; “Advanced Exposure-Time Calculations: Undersampling, Dithering, Cosmic Rays, Astrometry, and Ellipticities”
- Blain, A.W., Smail, I., Ivison, R.J., Kneib, J.-P. & Frayer, D.T. 2002, *PhRep*, 369, pp.111-176; “Submillimeter Galaxies”
- de Korte, P.A.J., Beyer, J., Deiker, S., Hilton, G.C., Irwin, K.D., Macintosh, M., Nam, S.W., Reintsema, C.D., Vale, L.R. & Huber, M.E. 2003, *RSI*, 74, pp. 3807-3815; “Time-division superconducting quantum interference device multiplexer for transition-edge sensors”
- Dicker, S.R., Abrahams, J.A., Ade, P.A.R., Ames, T.J., Benford, D.J., Chen, T.C., Chervenak, J.A., Devlin, M.J., Irwin, K.D., Komgut, P.M., Maher, S.F., Mason, B.S., Mello, M., Moseley, S.H., Norrod, R.D., Shafer, R.A., Staguhn, J.G., Talley, D.J., Tucker, C., Werner, B.A. & White, S.D. 2006, *Proc. SPIE #6275*, pp. 62751B; “A 90-GHz bolometer array for the Green Bank Telescope”
- Forgione, J.B., Benford, D.J., Buchanan, E.D., Moseley, S.H., Rebar, J. & Shafer, R.A. 2004, *Proc. SPIE #5498*, pp. 784-795; “Enhancements to a superconducting quantum interference device (SQUID) multiplexer readout and control system”
- Glenn, J., Ade, P.A.R., Amarie, M., Bock, J.J., Edgington, S.F., Goldin, A., Golwala, S., Haig, D., Lange, A.E., Laurent, G., Mauskopf, P.D., Yun, M. & Nguyen, H. 2003, *Proc. SPIE #4855*, pp.30-40; “Current status of Bolocam: a large-format millimeter-wave bolometer camera”
- Holland, W., Macintosh, M., Fairley, A., Kelly, D., Montgomery, D., Gostick, D., Atad-Etiedgui, E., Ellis, M., Robson, I., Hollister, M., Woodcraft, A., Ade, P., Walker, I., Irwin, K., Hilton, G., Duncan, W., Reintsema, C., Walton, A., Parkes, W., Dunare, C., Fich, M., Kycia, J., Halpern, M., Scott, D., Gibb, A., Molnar, J., Chapin, E., Bintley, D., Craig, S., Chylek, T., Jenness, T., Economou, F. & Davis, G. 2006, *Proc. SPIE #6275*, pp.62751E; “SCUBA-2: a 10,000-pixel submillimeter camera for the James Clerk Maxwell Telescope”
- Kreysa, E., Gemünd, H.-P., Raccanelli, A., Reichertz, L. A. & Siringo, G. 2002, *AIPC*, 616, 262; “Bolometer arrays for Mm/Submm astronomy”
- Staguhn, J.G., Benford, D.J., Chervenak, J.A., Moseley, S.H., Jr., Allen, C.A.; Stevenson, T.R.; Hsieh, W.-T., 2004, *Proc. SPIE #5498*, pp. 390-395; “Design techniques for improved noise performance of superconducting transition edge sensor bolometers”
- Staguhn, J.D., Benford, D.J., Allen, C.A., Moseley, S.H., Sharp, E.H., Ames, T.J., Brunswig, W., Chuss, D.T., Dwek, E., Maher, S.F., Marx, C.T., Miller, T.M., Navarro, S. & Wollack, E.J. 2006, *Proc. SPIE #6275*, pp.62751D; “GISMO: a 2-millimeter bolometer camera for the IRAM 30 m telescope”
- Willott, C. J., McLure, R. L. & Jarvis, M. J. 2003, *ApJ*, 587, pp. L15-L18; “A $3 \times 10^9 M_{\text{solar}}$ Black Hole in the Quasar SDSS J1148+5251 at $z=6.41$ ”